NJC

Direct Catalytic Benzene Hydroxylation under Mild Reaction Condition by Using a Monocationic μ-Nitrido-Bridged Iron Phthalocyanine Dimer with 16 Peripheral Methyl Groups

Journal:	*New Journal of Chemistry*
Manuscript ID	NJ-COM-11-2021-005369.R1
Article Type:	Communication
Date Submitted by the Author:	11-Dec-2021
Complete List of Authors:	Yamada, Yasuyuki; Nagoya University, Research Center for Materials Science Teoh, Chee-Ming; Nagoya University, Department of Chemistry, Faculty of Science Toyoda, Yuka; Nagoya University, Department of Chemistry Tanaka, Kentaro; Nagoya University, Department of Chemistry, Graduate School of Science

COMMUNICATION

Direct Catalytic Benzene Hydroxylation under Mild Reaction Condition by Using a Monocationic μ-Nitrido-Bridged Iron Phthalocyanine Dimer with 16 Peripheral Methyl Groups

Received 00th January 20xx,
Accepted 00th January 20xx

DOI: 10.1039/x0xx00000x

Yasuyuki Yamada,*[a,b,c] Chee-Ming Teoh,[a] Yuka Toyoda,[b] and Kentaro Tanaka *[a]

Direct catalytic hydroxylation of benzene under mild reaction conditions proceeded efficiently in the presence of a monocationic μ-nitrido-bridged iron phthalocyanine dimer with 16 peripheral methyl groups in an acetonitrile solution with excess H_2O_2. Mechanistic studies suggested that the reaction was catalyzed by a high-valent iron-oxo species generated *in situ*. Moreover, the peripheral methyl groups of the catalyst were presumed to have enhanced the production rate of the iron-oxo species.

The conversion of benzene to phenol is an important process in the chemical industry. The cumene process, shown in Figure 1a, is the most widely used method for producing phenol. It is considered an energy-intensive process because it requires benzene to undergo multiple chemical reactions at high temperatures and pressures.[1,2] In contrast, the direct C-H bond hydroxylation of benzene (Figure 1b) under mild reaction conditions is a more energy-efficient process and is considered as a good alternative to the cumene process for phenol production. However, it is difficult to introduce a hydroxyl group to benzene directly because the reactivity of aromatic C-H bond of benzene is low. Therefore, significant research efforts have been devoted toward the exploration of potential catalysts for the efficient and low-energy C-H bond hydroxylation of benzene.[3–13]

Molecular oxidation catalysts are well recognized as promising tools for direct benzene hydroxylation because their activities can be fine-tuned using an appropriate combination of metals and ligands.[8–13] Among a variety of oxidation catalysts, a μ-nitrido-bridged iron phthalocyanine dimer, wherein the N atom bridges the Fe centers of two iron phthalocyanines, is an interesting candidate for direct benzene hydroxylation.[13] This is primarily because it is one of the few molecular catalysts that can also be used for the direct C-H bond hydroxylation of methane at temperatures lower than 100 °C in the presence of H_2O_2.[14–19] As shown in Figure 1c, both of a neutral species **1** possessing a Fe(III) and a Fe(IV) cores and a monocationic species $\mathbf{1}^+$ having two Fe(IV) cores show high catalytic activities.[14,15,19] The reactive intermediate is a high-valent iron-oxo species ($\mathbf{1}_{oxo}$) that can be generated by reacting with H_2O_2, as illustrated in Figure 1c.[15,17]

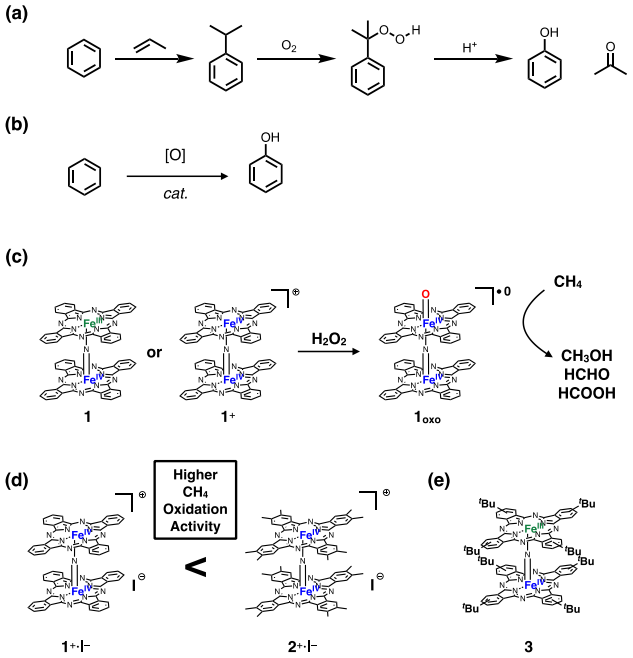

Figure 1. Reaction schemes of the (a) cumene process and (b) direct benzene hydroxylation. (c) Formation of high-valent iron-oxo species $\mathbf{1}_{oxo}$ from **1** or $\mathbf{1}^+$. (Refs. 15, 16, 19) (d) Methane oxidation activity of $\mathbf{1}^+\cdot I^-$ and $\mathbf{2}^+\cdot I^-$. (e) Neutral μ-nitrido-bridged iron phthalocyanine dimer that catalyzes benzene hydroxylation. (Ref. 13)

We recently reported that the introduction of 16 electron-donating methyl groups on the periphery of a monocationic μ-nitrido-bridged iron phthalocyanine dimer significantly increases methane oxidation reactivity.[19] Turnover number (TON) for methane oxidation by $\mathbf{2}^+\cdot I^-$ was found to be more than 7 times higher than that

[a] Department of Chemistry, Graduate School of Science, Nagoya University, Furo-cho, Chikusa-ku, Nagoya 464-8602, Japan.
[b] Research Center for Materials Science, Nagoya University, Furo-cho, Chikusa-ku, Nagoya 464-8602, Japan.
[c] JST, PRESTO, 4-1-8 Honcho, Kawaguchi, Saitama, 332-0012, Japan.
†E-mail: yy@chem.nagoya-u.ac.jp, kentaro@chem.nagoya-u.ac.jp
Electronic Supplementary Information (ESI) available: [details of any supplementary information available should be included here]. See DOI: 10.1039/x0xx00000x

by $\mathbf{1}^{+}$ (Figure 1d). Considering that $\mathbf{2}^{+}\cdot I^{-}$ is one of the most effective molecular iron-oxo-based catalysts for methane oxidation and that a neutral μ-nitrido-bridged iron phthalocyanine dimer with eight *tert*-butyl moieties (**3**, Figure 1e) acts as a benzene oxidation catalyst, we became interested in the investigation of the catalytic benzene hydroxylation activity of a monocationic species $\mathbf{2}^{+}$.

Compound $\mathbf{2}^{+}\cdot I^{-}$ was synthesized using the method employed in our previous report.[19] Acetonitrile (CH_3CN) was utilized in this study as a solvent for benzene oxidation because of its inertness. Due to the low solubility of $\mathbf{2}^{+}\cdot I^{-}$ in several organic solvents including CH_3CN, the reaction was carried out using a silica-gel-supported catalyst ($\mathbf{2}^{+}\cdot I^{-}/SiO_2$).

Benzene oxidation was performed in a CH_3CN solution containing excess amounts of benzene (481 mM), trifluoroacetic acid (TFA, 132 mM), and H_2O_2 (983 mM) at 40 °C in the presence of $\mathbf{2}^{+}\cdot I^{-}/SiO_2$ (47 μM as $\mathbf{2}^{+}$). The oxidation by μ-nitrido-bridged iron phthalocyanine dimers requires an acidic condition to efficiently produce high-valent iron-oxo species.[14–21] The reaction was monitored and evaluated by ^{1}H-NMR spectroscopy. As shown in Figure S3 in the Supporting Information, a significant amount of phenol (5.04 mM, TON = 106) was produced after oxidation for 8 h. *p*-Quinone was observed in a low concentration, whereas other forms of overoxidized products including *o*-quinone, 1,2-, 1,3-, or 1,4-dihydroxybenzenes were not found in this reaction condition. It is considered that HCOOH, whose peak was observed in the NMR spectrum, was derived from CH_3CN because $\mathbf{2}^{+}\cdot I^{-}$ possesses high oxidizing ability that can oxidize chemically inert methane under similar reaction conditions.[19] Our attempt to oxidize benzene using H_2O as a solvent instead of CH_3CN (a two-phase reaction; see Supporting Material page S6) resulted in the generation of significantly lower amounts of the oxidized products than the reaction using CH_3CN. This is presumed to be caused by benzene's low solubility in H_2O.

The time dependence of the phenol concentration in the reaction at 40 °C is shown in Figure 2 and the results are summarized in Table 1. The increase in the phenol concentration was observed to be almost linear at least in the initial 32 h of oxidation. This suggests that $\mathbf{2}^{+}\cdot I^{-}$ stably catalyzed benzene oxidation. The amount of *p*-quinone was also found to be very low but gradually increased with phenol concentration in the reaction mixture. Low yields of *p*-quinone were

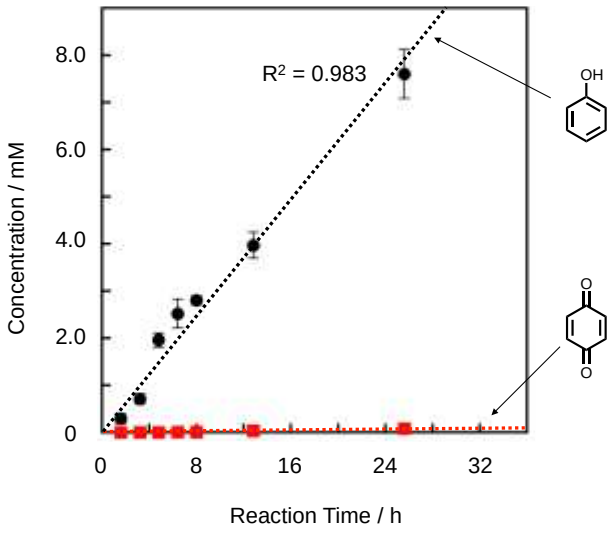

Figure 2. Time dependence of the concentrations of phenol (filled circle) and *p*-quinone (red square) observed in the reaction performed at 40 °C. Error bars indicate standard deviations of three independent reactions.

due to the significantly higher concentration of benzene than that of phenol produced during the oxidation reaction. At elevated temperatures (60 and 80 °C), the concentrations of the overoxidized products such as *p*-quinone, maleic acid, oxaloacetic acid, and formic acid also increased significantly, as shown in Figure S4 and Figure S5. This indicates that the benzene ring decomposed gradually.

The initial oxidation rates of several benzene derivatives were compared and examined as shown in Figure 3a to further understand the benzene oxidation reaction mechanism by $\mathbf{2}^{+}\cdot I^{-}$. As shown in Figure 3b, a linear correlation with a negative slope was observed in the Hammett plot,[22] which indicates the electrophilicity of the reactive species. The kinetic isotope effects (KIE) were also examined by comparing the initial oxidation rates of benzene (C_6H_6) and deuterated benzene (C_6D_6). The obtained KIE value (k_H/k_D) was 1.14 (for detail, see Supporting Information), which suggests that the C-H bond cleavage process is not involved in the rate-limiting step of the reaction. Moreover, the active species during benzene oxidation is

Table 1. Amounts of the oxidized products observed in the benzene oxidation reactions by using $\mathbf{2}^{+}\cdot I^{-}/SiO_2$ as a catalyst and turn over numbers (TONs) calculated from the concentration of phenol. N.d. indicates "not detected".

Entry	Catalyst	Reaction time / h	Temperature / °C	Additive	[Phenol] / mM	[*p*-Quinone] / mM	TON for PhOH production
1	$\mathbf{2}^{+}\cdot I^{-}/SiO_2$	2	40	···	0.58	n.d.	12
2	$\mathbf{2}^{+}\cdot I^{-}/SiO_2$	4	40	···	1.42	n.d.	30
3	$\mathbf{2}^{+}\cdot I^{-}/SiO_2$	6	40	···	3.92	n.d.	83
4	$\mathbf{2}^{+}\cdot I^{-}/SiO_2$	8	40	···	5.04	0.01	106
5	$\mathbf{2}^{+}\cdot I^{-}/SiO_2$	10	40	···	5.60	0.02	119
6	$\mathbf{2}^{+}\cdot I^{-}/SiO_2$	16	40	···	7.94	0.07	168
7	$\mathbf{2}^{+}\cdot I^{-}/SiO_2$	32	40	···	15.2	0.16	322
8	$\mathbf{2}^{+}\cdot I^{-}/SiO_2$	8	60	···	17.6	0.51	373
9	$\mathbf{2}^{+}\cdot I^{-}/SiO_2$	8	60	11.3 mM DMPO	18.8	0.47	397
10	$\mathbf{2}^{+}\cdot I^{-}/SiO_2$	8	80	···	26.0	0.74	568
11	$\mathbf{1}^{+}\cdot I^{-}/SiO_2$	6	40	···	0.41	0	8

not a hydroxyl radical (•OH) because the KIE values of a typical Fenton-type reaction are 1.7–1.8.[23] The benzene oxidation in the presence of 5,5-dimethyl-1-pyrroline-*N*-oxide (DMPO), a well-known radical scavenger,[6,9] was barely quenched, as shown in Table 1 (Entry 9). These results imply that high-valent iron-oxo species $\mathbf{2}_{oxo}$ generated from $\mathbf{2}^{+}$ should be the reactive intermediate, as shown in Figure 4, as in the case of methane oxidation.[19] Our attempt to detect the high-valent iron-oxo species ($\mathbf{2}_{oxo}$) directly was unsuccessful because of the low solubility of $\mathbf{2}^{+}\cdot I^{-}$ in many of stable solvents against oxidation.[17,21]

The oxidation by high-valent iron-oxo species generally proceeds through the proton-coupled electron transfer (PCET) mechanism,

(a)

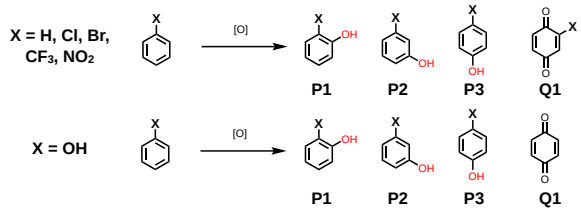

Entry	Benzene derivative	P1 / mM	P2 / mM	P3 / mM	Q1 / mM	Total amount (P1 + P2 + P3 +)	TON (Total)
1	PhOH (X = OH)	3.82	n.d.	0.60	4.52	8.94	189
2	PhH (X = H)	3.92	•••	•••	n.d.	3.92	83
3	PhCl (X = Cl)	1.18	0.34	0.65	n.d.	2.14	46
4	PhBr (X = Br)	0.63	0.04	0.69	n.d.	1.81	29
5	$PhCF_3$ ($X = CF_3$)	0.27	0.29	0.20	n.d.	0.66	16
6	$PhNO_2$ ($X = NO_2$)	0	0.46	0.21	n.d.	0.67	14

(b)

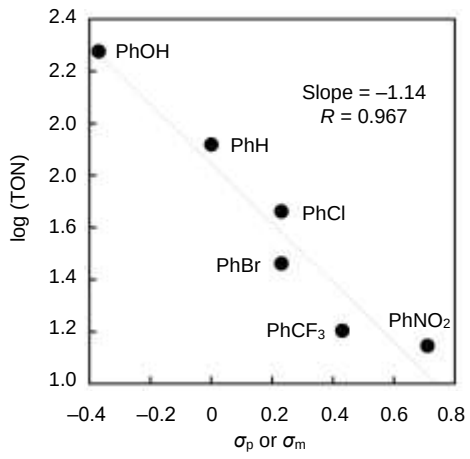

Figure 3. (a) Amounts of the oxidized products observed in the oxidations of benzene derivatives by using $\mathbf{2}^{+}\cdot I^{-}/SiO_2$ as a catalyst and turn over numbers (TONs) calculated from the total concentration of the oxidized products. N.d. indicates "not detected" in the ^{1}H-NMR measurement. The reactions were performed at 40 °C for 6 h. The ^{1}H-NMR spectra used for quantitative analyses of the oxidized compounds are shown in Figures S6–S10. (b) A Hammett plot of the TON for the oxidation of benzene derivatives. In the Hammett plot, the following substrates were used: PhOH (σ_p = –0.37), PhH (σ_p = 0.00), PhCl (σ_p = 0.23), PhBr (σ_p = 0.23), $PhCF_3$ (σ_m = 0.43), $PhNO_2$ (σ_m = 0.78). (Ref. 22)

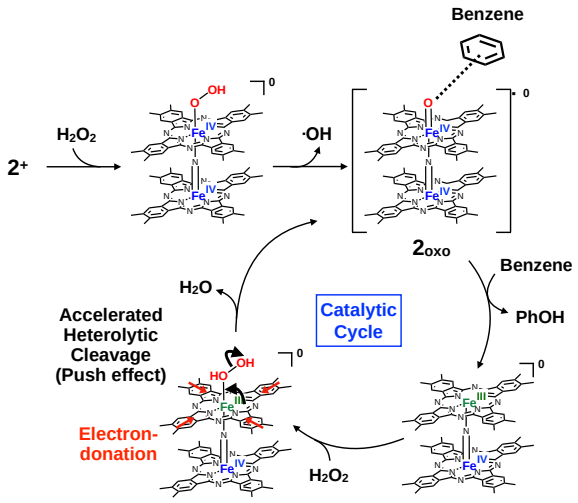

Figure 4. Proposed reaction mechanism of the benzene oxidation by $\mathbf{2}^{+}\cdot I^{-}$.

wherein proton and electron abstractions from the substrate are essential.[24,25] The obtained results shown in Figure 3b imply that the abstraction of the π-electron of the benzene ring by high-valent iron-oxo species could be involved in the rate-limiting step of benzene oxidation, while the opposite is observed for the proton abstraction process. Sorokin *et al.* suggested that benzene oxidation by **3** involved an epoxidation process of benzene ring.[13,26] It is also probable that the epoxidation is involved in the benzene oxidation by $\mathbf{2}_{oxo}$ because the kinetic isotope effect data for benzene hydroxylation by $\mathbf{2}^{+}$ was also compatible with the epoxidation mechanism.

The benzene hydroxylation rate of $\mathbf{2}^{+}\cdot I^{-}$ was also compared with that of $\mathbf{1}^{+}\cdot I^{-}$ having no peripheral substituents. It was found that the catalytic activity for phenol production by $\mathbf{2}^{+}\cdot I^{-}$ at 40 °C is approximately 10 times higher than that of $\mathbf{1}^{+}\cdot I^{-}$, as shown in Table 1. The degree of enhancement is comparable to that observed for methane oxidation reactions, which was approximately 7 times higher based on TON of $\mathbf{2}^{+}\cdot I^{-}$ compared to that of $\mathbf{1}^{+}\cdot I^{-}$.[19] The increase in the oxidation rate of the organic substrate by the introduction of electron-donating methyl groups on the periphery of a μ-nitrido-bridged iron phthalocyanine dimer was possibly caused by (1) the rise in the basicity of the oxygen atom of the high-valent iron-oxo species, which accelerated proton abstraction and (2) the increase in the production rate of the oxo-species, which promoted the heterolytic cleavage of the O-O bond of the hydroperoxo species of **2** by electron donation (push effect).[27] Actually, DFT calculation by de Vissel and Sorokin indicated that basicity of the high-valent iron-oxo species of a μ-nitrido-bridged iron phthalocyanine dimer could be increased by introduction of peripheral electron-donating substituents in the case of methane oxidation.[18] However, considering that kinetic isotope effect experiment indicated that hydrogen abstraction was not necessarily involved in the rate-limiting step in the benzene oxidation by $\mathbf{2}^{+}\cdot I^{-}$, the enhancement could be primarily attributed to the above-mentioned (2), as shown in Figure 4, although exact determination of the production rate of the oxo species was difficult because both of the catalase reaction,

where the iron-oxo species converts H_2O_2 into O_2, and low solubility of $\mathbf{2}^{+}\cdot I^{-}$.

In conclusion, this study investigated the benzene hydroxylation reaction using a monocationic μ-nitrido-bridged iron phthalocyanine dimer with 16 peripheral methyl groups ($\mathbf{2}^{+}\cdot I^{-}$) as a catalyst. The results showed that efficient hydroxylation proceeded at 40 °C and confirmed that the introduction of 16 methyl groups on the periphery of a monocationic μ-nitrido-bridged iron phthalocyanine dimer core increased the benzene hydroxylation rate. The push effect of the methyl moieties was presumed to have increased the production rate of the reactive iron-oxo species. These findings demonstrate the effectiveness of monocationic μ-nitrido-bridged iron phthalocyanine dimers as potent oxidation catalysts for various inert organic substrates.

Author Contributions

Y.Y conceived the project, designed the experiments, synthesized the catalyst, and analyzed the data. C.-M.T synthesized the catalysts, performed the oxidation reactions, and analyzed the data. Y.T. synthesized the catalyst and analyzed the data. Y.Y., C.-M. T, and K.T. cowrote the manuscript. All authors discussed the results and commented on the manuscript.

Conflicts of interest

There are no conflicts to declare.

Acknowledgements

This work was financially supported by a JSPS KAKENHI Grant-in-Aid for Scientific Research (B) (Number 19H02787), JST PRESTO (Number JK114b), Foundation of Public Interest of Tatematsu for YY, and a JSPS KAKENHI Grant-in-Aid for Scientific Research (A) (Number 19H00902) to KT.

Notes and references

1 R. J. Schmidt, *Appl. Catal., A*, 2005, **280**, 89-103.

2 R. Molinari, T. Poerio, *Asia-Pac. J. Chem. Eng.*, 2010, **5**, 191–206.

3 T. Jiang, W. Wang, B. Han, *New J. Chem.*, 2013, **37**, 1654–1664.

4 S. Fukuzumi, K. Ohkubo, *Asian J. Org. Chem.*, 2015, **4**, 836–845.

5 B. E. R. Snyder, M. L. Bols, R. A. Schoonheydt, B. F. Sels, E. I. Solomon, *Chem. Rev.*, 2018, **118**, 2718–2768.

6 M. Yamada, K. D. Karlin, S. Fukuzumi, *Chem. Sci.*, 2016, **7**, 2856–2863.

7 M. Karasawa, J. K. Stanfield, S. Yanagisawa, O. Shoji, Y. Watanabe, *Angew. Chem. Int. Ed.*, 2018, **57**, 12264–12269.

8 Y. Morimoto, S. Bunno, N. Fujieda, H. Sugimoto, S. Itoh, *J. Am. Chem. Soc.*, 2015, **137**, 5867–5870.

9 T. Tsuji, A. A. Zaoputra, Y. Hitomi, K. Mieda, T. Ogura, Y. Shiota, K. Yoshizawa, H. Sato, M. Kodera, *Angew. Chem. Int. Ed.*, 2017, **56**, 7779–7782.

10 Y. Gu, Q. Li, D. Zang, Y. Huang, H. Yu, Y. Wei, *Angew. Chem. Int. Ed.*, 2021, **60**, 13310–13316.

11 S. Muthuramalingam, K. Anandababu, M. Velusamy, R. Mayilmurugan, *Inorg. Chem.*, 2020, **59**, 5918–5928.

12 S. Kumari, S. Muthuramalingam, A. K. Dhara, U. P. Singh, R. Mayilmurugan, K. Ghosh, *Dalton Trans.*, 2020, **49**, 13829–13839.

13 E. V. Kudrik, A. B. Sorokin, *Chem. Eur. J.*, 2008, **14**, 7123–7126.

14 A. B. Sorokin, E. V. Kudrik, L. X. Alvarez, P. Afanasiev, J. M. M. Millet, D. Bouchu, *Catal. Today*, 2010, **157**, 149–154.

15 P. Afanasiev, A. B. Sorokin, *Acc. Chem. Res.*, 2016, **49**, 583–593.

16 A. B. Sorokin, E. V. Kudrik, D. Bouchu, *Chem. Commun.*, 2008, 2562–2564.

17 E. V. Kudrik, P. Afanasiev, L. X. Alvarez, P. Dubourdeaux, M. Clémancey, J.-M. Latour, G. Blondin, D. Bouchu, F. Albrieux, S. E. Nefedov, A. B. Sorokin, *Nat. Chem.*, 2012, **4**, 1024–1029.

18 Ü. ís¸ci, A. S. Faponle, P. Afanasiev, F. Albrieux, V. Briois, V. Ahsen, F. Dumoulin, A. B. Sorokin, S. P. de Visser, *Chem. Sci.*, 2015, **6**, 5063–5075.

19 Y. Yamada, J. Kura, Y. Toyoda, K. Tanaka, *Dalton Trans.*, 2021, **50**, 6718–6724.

20 Y. Yamada, K. Morita, N. Mihara, K. Igawa, K. Tomooka, K. Tanaka, *New J. Chem*., 2019, **43**, 11477–11482.

21 N. Mihara, Y. Yamada, H. Takaya, Y. Kitagawa, K. Igawa, K. Tomooka, H. Fujii, K. Tanaka, *Chem. Eur. J*., 2019, **25**, 3369–3375.

22 C. Hansch, A. Leo, R. W. Taft, *Chem. Rev.*, 1991, **91**, 165–195.

23 R. Augusti, A. O. Dias, L. L. Rocha, R. M. Lago, *J. Phys. Chem. A*, 1998, **102**, 10723–10727.

24 D. R. Weinberg, C. J. Gagliardi, J. F. Hull, C. F. Murphy, C. A. Kent, B. C. Westlake, A. Paul, D. H. Ess, D. G. McCafferty, T. J. Meyer, *Chem. Rev.*, 2012, **112**, 4016–4019.

25 J. E. M. N. Klein, G. Knizia, *Angew. Chem. Int. Ed.*, 2018, **57**, 11913–11917.

26 C. Colomban, E. V. Kudrik, P. Afanasiev, A. B. Sorokin, *J. Am. Chem. Soc.,* 2014, **136**, 11321–11330.

27 K. Yamaguchi, Y. Watanabe, I. Morishima, *Inorg. Chem.*, 1992, **31**, 156–157.